Sensors & Transducers, Vol. 158, Issue 11, November 2013, pp. 27-32

www.sensorsportal.com

Sensors & Transducers

http://www.sensorsportal.com

Mechanism Analysis and Simulation of Coplanar Multi-Electrode Capacitive Ice Thickness Measuring Sensor

[1] Dou YINKE, [2] Chang XIAOMIN

[1] College Electric and Power Engineering of Taiyuan University of Technology, 030024, Tai Yuan, China

[2] Key Laboratory of Advanced Transducers and Intelligent Control System, Ministry of Education, Taiyuan, 030024, China

E-mail: douyinke@yeah.net

Received: 10 September 2013 /Accepted: 25 October 2013 /Published: 30 November 2013

Abstract: In this paper, we use the coplanar multi-electrode for designing a rod-shaped sensor for measuring the ice thickness. In order to analyze and study mechanism and feasibility of ice thickness measurements using this technique, we use modes of mathematical model derivation and software simulation to study coplanar multi-electrode capacitance sensors. It uses MAXWELL software to simulate the coplanar multi-electrode capacitance sensor under the models which are being approached by three different media, namely ice, air and water. Both mathematical model derivation and simulation results show that the sensor designed with coplanar multi-electrode capacitance can be used to level the automated measurement of sea ice or river ice thickness. The accuracy is ± 1 cm. *Copyright © 2013 IFSA.*

Keywords: Coplanar multi-electrode capacitive, Simulation, Ice thickness, Simulation, Sensor.

1. Introduction

Ice thickness and its change process is one of the basic factors for the study of ice generation and disappearance, ice jam and ice jam flood. Sea ice thickness is the most basic and important parameter to simulate the state of the sea ice [1]. Monitoring the thickness of sea ice is an important tool in assessing the impact of global warming on Earth's Polar Regions [2]. It is also a difficult problem to realize real-time automatic monitor of fixed-point ice thickness continuously. At present, the application of ice thickness and ice detection technology under the water level can be summarized into three types. The first type is to measure directly by drilling holes artificial. The second one is satellite remote sensing [3], radar [4], a combination of electromagnetic induction and laser ranging techniques [5, 6], shipboard sonar and other equipment [7, 8], which can measure the medium and large scale sea ice thickness. The third one is the electromagnetic physical detection, such as ultrasonic [9] detection method whose fatal flaw is big error, etc.

According to actual demand of the sea ice measurement [10, 11], the designed ice thickness sensor is consist of many electrodes (more than 100, each electrode shows 1 cm), and many electrode was arranged in the same plane evenly. This sensor is also a uniplanar diffused capacitive sensor, a kind of electric field-leaked sensor [12, 13]. When detects, one of the electrode was excited and all other electrodes were grounded [14]. Fig. 1 is a part of uniplanar polyelectrode sensor, No. 3 of the 5 electrodes was excited by the excitation power and all other electrodes were grounded. Fig. 3 is the sketch map of the power line when the No. 3

electrode was approached by the medium. From the figure, except for the virtual earth capacitance C3 consist of the excitation electrode 3 and the ground, the excitation electrode also combined the uniplanar grounded capacitance to form a capacitance, so the equivalent capacitance electric circuit was showed in Fig. 2, which consist of 3 paralleling capacitances. C1 and C2 are equivalent capacitance of the uniplanar electrodes. Because when detects, all electrodes are exciting electrodes and each electrode has different position in the uniplanar polyelectrode, which means all electrode has different number of grounding electrode on the left and right when serves as exciting electrode, so C1 is not equivalent to C2 generally. When different dielectricity material approached the exciting electrode, C1, C2, C3 all changes and all three capacitive parallel connected [15]. If we consider the changed electric capacity as C_x, thus C_x=C1+C2+C3, the electric voltage of point A changed in directly proportional with 1/Cx. We change the detected electric voltage of point A through internal amplitude detector and low-pass filter to DC sign, and deal the sign through micro-controller with A/D controller as Single-Chip computer to execute function of any numbers to achieve the measurement.

In this paper, we first derive mathematical models of coplanar multi-electrode and capacitive sensors, and then propose the principle of ice thickness measurement using coplanar multi-electrode capacitive sensors. Finally, we use MAXWELL software for simulation of the measurement mechanism.

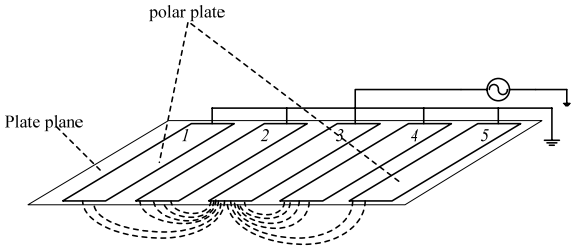

Fig. 1. Model of the uniplanar capacitance sensor with multi-electrode.

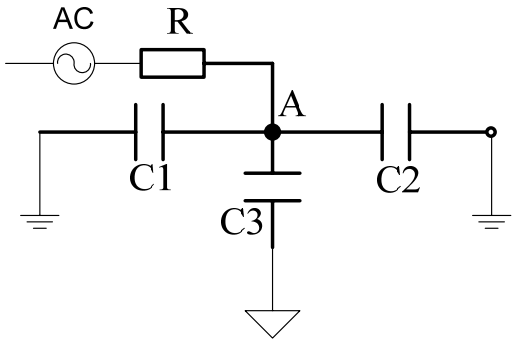

Fig. 2. The equivalent circuit of a plane with multi-electrode capacitance.

2. Principle of Coplanar Multi-Electrode Capacitive Ice Thickness Detect Sensor

2.1. Calculation of Coplanar Multi-Electrode Equivalent Capacitance

In the individual electrode plate, set the length to A and the width to B. The spacing of the adjacent electrode plates is L. When the intermediate electrode connects the sine-wave excitation source, two pieces of electrodes around are grounded. At this time, the idealized power line is shown as in Fig. 3, with the approximate arc replacing the actual power line. The positive axis of Y-axis is the working interval, while the capacitance formed in the left and right working area is equivalent. For easy calculation, select the capacitance formed by the electric field in the right half to create coordinate calculations [16].

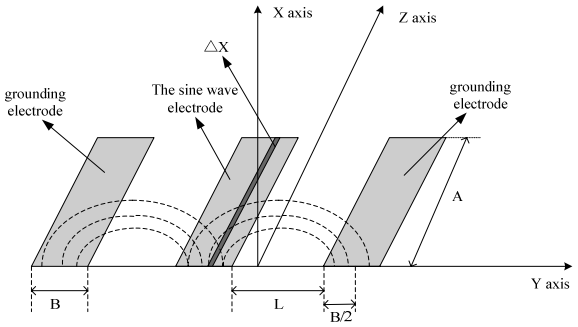

Fig. 3. Distribution map of ideal distribution power lines when the excitation is applied to the coplanar multi-electrode sensor.

From the minor area increment $\Delta S = A \times \Delta x$ of the capacitance sensing element, take the capacitance value ΔC_x generated, Δx is the small increment unit in the X direction [17]. As shown in Figs. 1-3, set the length of the semicircular arc power line to *d*. According to the formula in the literature searched, we have:

$$\Delta C_x \approx \frac{\varepsilon_x \cdot \Delta S}{d} = \frac{\varepsilon_x \cdot A \cdot \Delta x}{\pi\left(X + \frac{L}{2}\right)} \tag{1}$$

When X is taken as integral from $0 \sim \frac{B}{2}$, we can get C_w, namely:

$$C_w \approx \int_0^{\frac{B}{2}} \frac{\varepsilon_x \cdot A}{\pi\left(X + \frac{L}{2}\right)} \cdot dx$$

$$= \frac{2 \cdot \varepsilon_x \cdot A}{\pi} \int_0^{\frac{B}{2}} \frac{1}{(2X + L)} \cdot dx \tag{2}$$

$$= \frac{\varepsilon_x \cdot A}{\pi} \cdot \ln \frac{L + B}{L}$$

The equivalent capacitance total between the resulting two electrodes is:

$$C = 2\frac{\varepsilon_x \cdot A}{\pi} \cdot \ln\frac{L+B}{L} \tag{3}$$

By equation (3), when the length of electrode is fixed, the electrode width and the distance between adjacent electrodes are main parameters influencing the size of capacitance. However, Equation (3) is only idealized derivation. The actual power line is not necessarily circular and may be oval or diverging. For example, when the electrode spacing is infinitely small, the electric capacity calculated this way is infinitely large. This is apparently not true. When the spacing is infinitely small, the distribution of power lines will be in straight-line distribution, and the formula for calculating capacitance will no longer be true. Therefore, the calculation of the equivalent capacitance above has a specific scope of application.

2.2. Principle

Fig. 4 is a mechanism block diagram of the capacitive sensing-type ice layer thickness instrument, which is mainly made up of measurement sensor and SCM.

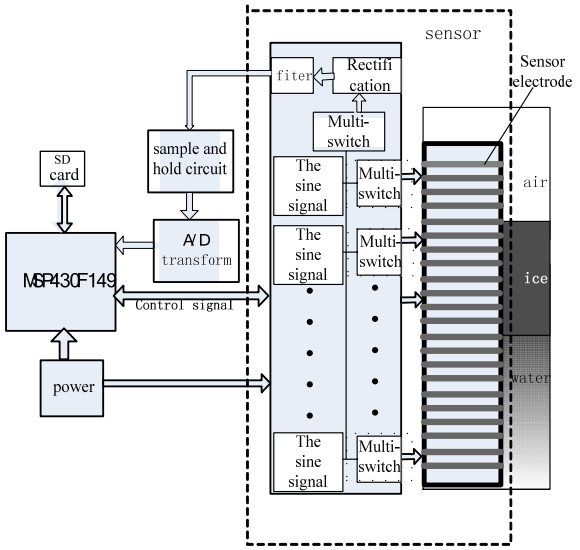

Fig. 4. Structure diagram of measurement system model.

The sensor is constituted by the external electric field sensing measuring electrode, multi-way analog switch circuits, sine signals generating circuit and the detecting and filtering circuit as well as the controlling circuit. Every set of sine signal generating circuits and multi-way analog switch circuits are designed in the same circuit board connecting 7 electrodes. In line with the different ice layer thicknesses, the system can design 1 m sensor, i.e. 100 external measuring electrodes; or 3 m sensor, i.e. 300 measuring electrodes. The multi-way analog switches capitalize on MC33993, whose major function is to conduct channel selection for every electrode in a move to measure the signal voltage values of different electrodes under the control of the SCM. Through channel selection, the voltage signal component measured by each electrode is sent to MSP430 SCM for processing and storage after A/D conversion with the signal acquisition circuit. Because every electrode is in different position of the sensor, the medium sensed by every electrode can only be ice, water or air. According to the measured data in every electrode, the ice layer thickness can be determined.

3. Digital Simulation

Using the Maxwell software, perform the simulation study on the scattered electric field distribution and the intensity variation rule when ice, water and air respectively approach the coplanar multi-electrode sensor. The simulation model is: Sequentially place 8 metal foil electrodes, with a length of 10 cm, a width of 6mm and a thickness of 0.2 mm, in parallel on the same plane, with each one spaced at a distance of 4 mm. The resin materials are adopted to cover both up and down the electrodes, wherein the thickness of epoxy resins over electrodes is 2 mm, and the thickness of epoxy resin under electrodes is 40 mm. The model uses 2D solver of Maxwell this time, so the following figure is a two-dimensional model. Select a section of the electrode section on the plane, with the coplanar multi-electrode sensor simulation model shown in Fig. 5.

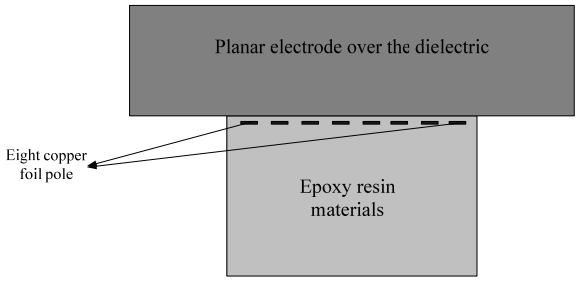

Fig. 5. Coplanar 8-electrode sensor simulation model.

In the coplanar 8-electrode sensor model, the measured substance is set over the electrodes, i.e., the measured substance is closely attached to the epoxy resin-sealed electrodes. The measured substances over the coplanar multi-electrode sensor model (rectangular area) are respectively set to ice (with a relative dielectric constant of 6), water (with a relative dielectric constant of 80) and air (with a relative dielectric constant of 1). The rectangular area under the electrodes is made of 40 mm-thick epoxy resin materials, and outside the model is a potential distribution around excitation electrodes when the

vacuum boundary exists. The potential distribution around the excitation electrode obtained by simulation is shown in Fig. 6.

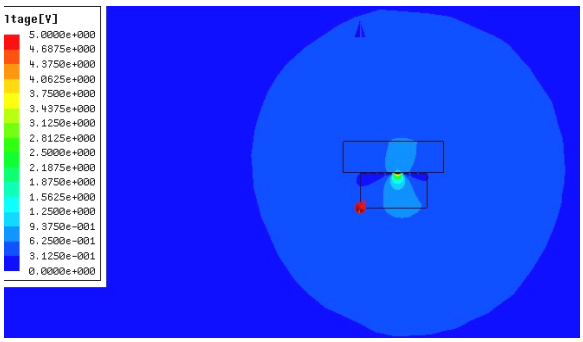

Fig. 6 (a). Voltage intensity distribution of water.

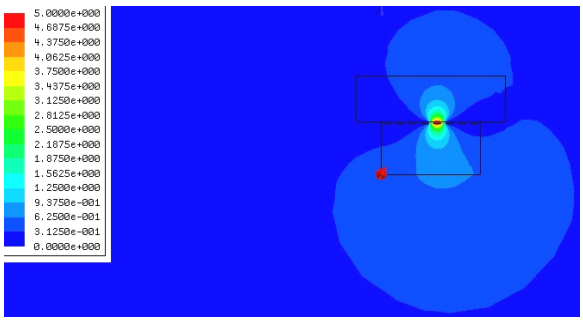

Fig. 6 (b). Voltage intensity distribution of air.

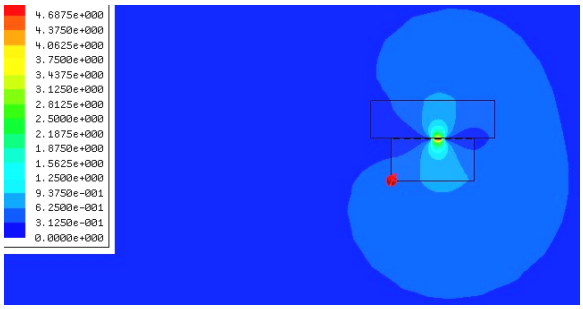

Fig. 6 (c). Voltage intensity distribution of ice.

From three electric field cloud diagrams, it can be seen that when the dielectric constant of measured substance is large (water), the electric field cloud graph over the excitation electrode is widely distributed and dispersed, which can basically fill a rectangular area above the electrode, but the yellow-green energy over the excitation electrode has a small area and a small electric field intensity; when the measured substance has a small dielectric constant, the electric field distribution right above the (air) excitation electrode is relatively concentrated and can not fill the rectangular area above the electrode. However, the yellow-green energy over the excitation electrode has a large area and a large electric field intensity; when the dielectric constant between the measured substance is between water and air (ice), the electric field distribution just above the excitation electrodes is just somewhere in between. The distribution is not as broad as when the medium is water, but stronger than air, able to fill most of the rectangular area above the electrodes. The yellow-green area above its excitation electrodes is also in between, with the electric field intensity being larger than in water but smaller than in air. It can also be seen that the size, shape and color of potential cloud graph under the excitation electrode (epoxy) always has no changes.

Fig. 6 only shows that the electric field intensity distributions of three kinds of different measured substances are significantly different. In order to further observe the information on electric field intensity above the excitation electrodes when the measured substance set above the electrodes are ice, water and air, the author uses the post-processing software of the Maxwell, to draw out the electric field intensity curve over the electrodes when the measured substances are separately ice, water and air, as shown in Fig. 7.

The horizontal coordinate of the graph is the overall length distance for the coplanar multi-electrode sensor model, in millimeters; the vertical coordinate gives the electric field intensity, in Newton/libraries.

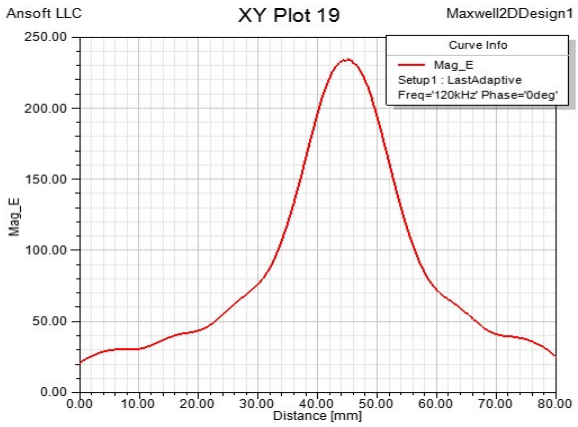

Fig. 7 (a). Electric field intensity distribution curve of ice.

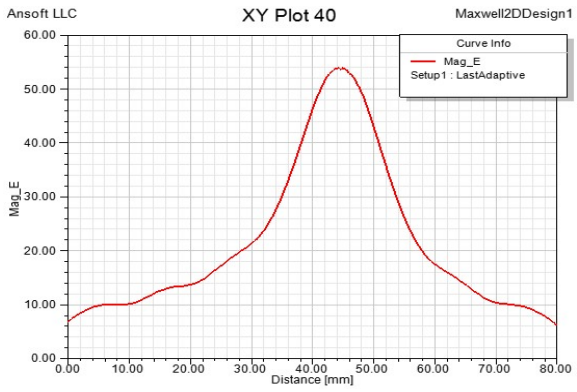

Fig. 7 (b). Electric field intensity distribution curve of water.

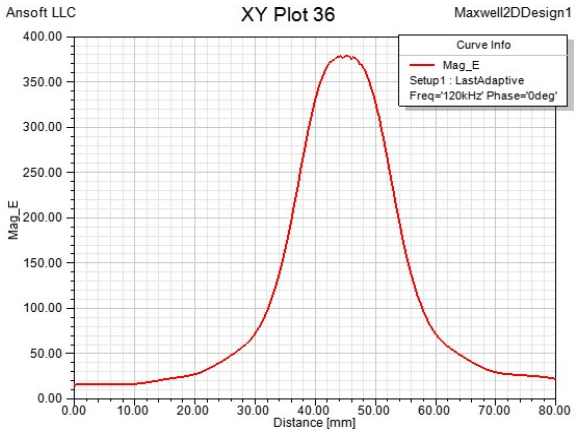

Fig. 7(c). Electric field intensity distribution curve of air.

As can be seen from Fig. 7, regardless of what the measured object above the electrode is set to, the electric field intensity above the excitation electrode is always the strongest, and the shape of the curve is basically consistent, with the overall curve taking on normal distribution, and the electric field intensity gradually waning from right above the excitation electrodes to both sides. When the measured substance is water, the electric field intensity right above the excitation electrode is the minimum, with its values at only around $54 N/C^{-1}$, while the speed at which the electric field intensity gradually decreases to two sides is slow, with gentle curve; when the measured substance is air, the electric field intensity right above the excitation electrode is the maximum, with its values at only around $380 N/C^{-1}$, while the speed at which the electric field intensity gradually decreases to two sides is quick, with steep curve; when the measured substance is ice, the electric field intensity right above the excitation electrode is between that for water and that for air, i.e., higher than that for water, and lower than that for air, its value being about $230 N/C^{-1}$, and speed at which the electric field intensity decreases to two sides is also in between, with the curve being relatively flat. As can be seen, the electric field energy is mainly concentrated just above the excitation electrode, while the size of the energy concentration area generally has no connection with the measured substance above the electrodes. Fig. 8 respectively depicts the electric field intensity cloud graph around the electrode 5 when medium is water, air and ice respectively.

As can be seen from the figure, when the measured substance is water, the electric fields around the excitation electrode are mainly distributed between the excitation electrodes and the measured substance; when the measured substance is air, the electric fields around the excitation electrode are mainly distributed between the excitation electrodes and two adjacent electrodes; when the measured material is ice, most of the electric field of the excitation electrode are distributed between the excitation electrode and the measured substance, with a small portion of the electric field is still located between the excitation electrode and the adjacent electrodes. As can be seen from several figures above, when dielectrics with different dielectric constants approach or contact the excitation electrodes, the electric field distribution around the electrodes are different, and its electric field intensity is also different.

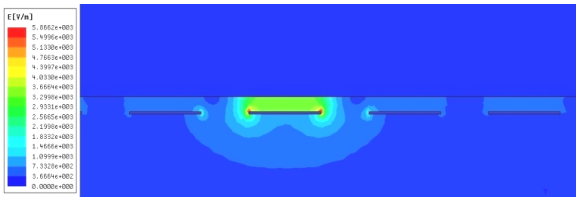

Fig. 8 (a). Electric field intensity cloud graph around the electrode 5 (the measured substance is water).

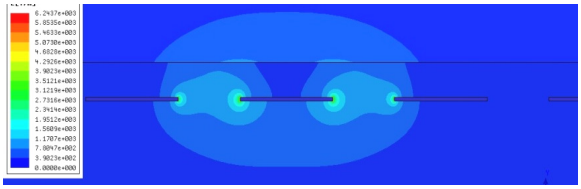

Fig. 8 (b). Electric field intensity cloud graph around the electrode 5 (the measured substance is air).

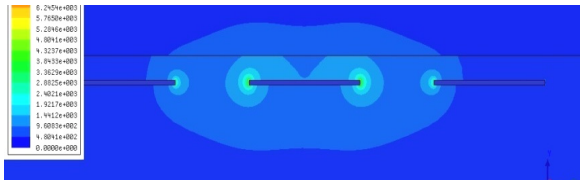

Fig. 8(c). Electric field intensity cloud graph around the electrode 5 (the measured substance is ice)

4. Conclusions

Through principle analysis and simulation of the coplanar multi-electrode capacitive ice measurement sensor, we can see that when the measured substance on the coplanar multi-electrode sensors are respectively air, ice and water, their electric field intensity variations are different to a very large extent. By indirectly measuring the electric field intensity, we can distinguish between measured substances, i.e., the sensor measuring ice thickness, which is designed and fabricated using such method, can be used for thickness measurement of leveled sea ice or river ice, providing basic data to the thermodynamic study of ice.

Acknowledgements

This study was supported by the National Natural Science Foundation of China (No. 41176080). And

supported by Shanxi Science and Technology research project (No. 20110321026-02). I would like to thank the Office of Science and Technology in Shanxi Province in this paper to give financial support.

References

[1]. W. Meier, J. Stroeve, F. Fetterer, K. Knowles, Reductions in arctic sea ice cover no longer limited to summer, *Eos Transactions of the American Geophysical Society,* Vol. 86, No. 36, 2005, pp. 3-26.

[2]. J. Zhu, K. M. Golden, A. Gully, C. Sampson, A network model for electrical transport in sea ice, *Physica B,* Vol. 405, 2010, pp. 3033-3036.

[3]. T. Tamura, K. I. Ohshima, T. Markus, et al., Estimation of thin ice thickness and detection of fast ice from SSM/I data in the Antarctic Ocean, *Journal of Atmospheric and Oceanic Technology*, Issue 24, 2007, pp. 1757-1772.

[4]. B. Sun, J. H. Wen, M. B. He, et al., Sea ice thickness measurement and its underside morphology analysis using radar penetration in the Arctic Ocean, *Science in China-D*, Vol. 46, Issue 11, 2003, pp.1151-1160.

[5]. C. Haas, Evaluation of ship-based electromagnetic-inductive thickness measurements of summer sea-ice in the Bellingshausen and Amundsen Seas, Antarctica, *Cold Regions Science and Technology*, Issue 27, 1998, pp. 1-16.

[6]. Christian Haas, John Lobach, Stefan Hendricks, Lasse Rabenstein, Andreas Pfaffling, Helicopter-borne measurements of sea ice thickness, using a small and lightweight, digital EM system, *Journal of Applied Geophysics,* Vol. 67, 2009, pp. 234-241.

[7]. D. A. Rothrock, Y. Yu, G. A. Maykut, Thinning of the Arctic sea-ice cover, *Geophysical Research Letters*, Vol. 26, Issue 23, 1999, pp. 3469-3472.

[8]. V. H. Strass, Measuring sea ice draft and coverage with moored upward looking sonars, *Deep-Sea Research I*, Vol. 45, 1998, pp. 795-818.

[9]. Marcel Nicolaus, Stephen R. Hudson, Sebastian Gerland, Karin Munderloh, A modern concept for autonomous and continuous measurements of spectral albedoand transmittance of sea ice, *Cold Regions Science and Technology*, Vol. 62, 2010, pp. 14-28.

[10]. J. L. Novak, J. J. Wiczer, A high-resolution capacitative imaging sensor for manufacturing applications, in *Proceedings of the IEEE International Conference on Robotics and Automation,* Vol. 3, 9–11 April 1991, pp. 2071-2078.

[11]. J. Novak, J. Feddema, A capacitance-based proximity sensor for whole arm obstacle avoidance, in *Proceedings of the International Conference on Robotics and Automation,* Vol. 2, Albuquerque, USA, May, 1992, pp. 1307-1314.

[12]. T. Perme, Introduction to Capacitive Sensing, *Microchip Technology*, *Inc.*, 2007, pp. 231-243.

[13]. T. Perme, Layout and physical design guidelines for capacitive sensing, *Microchip Technology, Inc.*, 2007.

[14]. Xiang Li, Dong Yonggui, Electrode structure and characteristics of uniplanar scattering-field capacitive sensors, *Journal of Tsinghua University (Science and Technology)*, Vol. 11, Issue 44, 2004, pp. 1471-1474.

[15]. Nathan Kirchner, Daniel Hordern, Dikai Liu, Gamini Dissanayake, Capacitive sensor for object ranging and material type identification, *Sensors and Actuators A,* Vol. 148, 2008, pp. 96-104.

[16]. Amr A. Nassr, Wael H. Ahmed, Wael W. EI-Dakhakhni, Coplanar capacitance sensor for detecting water intrusion in composite structures, *Measurement Science Technology*, Vol. 19, 2008, pp. 675-702.

[17] W. EI-Dakhahni, W. H. Ahmed, Capacitance sensors for detecting damage in composites, *US Provisional Patent Application,* No. 60/614055, 2004.